# Acoustic wave propagation in gassy porous marine sediments: The rheological and the elastic effects

Hakan Dogan, Paul R. White, and Timothy G. Leighton[a)]

*Institute of Sound and Vibration Research, University of Southampton, Highfield, Southampton SO17 1BJ, United Kingdom*

The preceding paper in this series [Mantouka, Dogan, White, and Leighton, J. Acoust. Soc. Am. **140**, 274–282 (2016)] presented a nonlinear model for acoustic propagation in gassy marine sediments, the baseline for which was established by Leighton [Geo. Res. Lett. **34**, L17607 (2007)]. The current paper aims further advancement on those two studies by demonstrating the particular effects of the sediment rheology, the dispersion and dissipation of the first compressional wave, and the higher order re-scattering from other bubbles. Sediment rheology is included through the sediment porosity and the definition of the contact interfaces of bubbles with the solid grains and the pore water. The intrinsic attenuation and the dispersion of the compressional wave are incorporated using the effective fluid density model [Williams, J. Acoust. Soc. Am. **110**, 2276–2281 (2001)] for the far field (fully water-saturated sediment). The multiple scattering from other bubbles is included using the method of Kargl [J. Acoust. Soc. Am. **11**, 168–173 (2002)]. The overall nonlinear formulation is then reduced to the linear limit in order to compare with the linear theory of Anderson and Hampton [J. Acoust. Soc. Am. **67**, 1890–1903 (1980)], and the results for the damping coefficients, the sound speed, and the attenuation are presented. © *2017 Acoustical Society of America*.
[http://dx.doi.org/10.1121/1.4978926]

## I. INTRODUCTION

In 1980, Anderson and Hampton[1,2] published what is still the dominant theory for acoustic propagation in gassy marine sediments. In 2007 Leighton[3] described acoustic propagation in gassy marine sediments where the bubbles could in addition behave in a nonlinear non-stationary manner—unlike the linear steady-state motions considered by Anderson and Hampton (the latter is abbreviated as A&H hereafter). Leighton further noted how the next stage would be to include radiation losses in this model, which was done by Mantouka *et al.*[4] The current paper aims further advancement on those two studies by demonstrating the particular effects of the sediment rheology (i.e., the shear viscosity and the rigidity), the dispersion and dissipation of the first compressional wave, and the higher order re-scattering from other bubbles.

Understanding the effect of gas on acoustic propagation is important, because extensive distributions of seafloor methane gas and hydrates have been detected at many locations around the world by geophysical surveys.[5] The importance of two-way gas transfer (both natural[6] and man-made[7]) between atmosphere, ocean, and seabed is becoming increasingly clear. The presence of gas affects the physical properties of the marine sediment, which is of interest for several applications including drilling operations, construction of seafloor structures, climate change, and the slope stability of sediments.[8] Furthermore, as part of future Carbon Capture and Storage (CCS) projects, the long term acoustic monitoring for possible greenhouse gas seepage in sub-seafloor reservoirs will be crucial.[9,10]

Biot[11,12] presented a model for the acoustic propagation in a porous two-phase medium. It has been validated for laboratory samples using ultrasonic frequencies,[13,14] and has been applied to sediment acoustics.[15–17] Many studies[18–23] attempted to establish modified versions of Biot theory to model the presence of gas bubbles in sediment pore spaces. These works have limited applicability to practical gas-bearing sediments because they assume the gas bubbles do not affect the sediment structure. The current paper joins the small canon of works[1–4,24,25] that model "sediment-replacing" bubbles,[26] to predict how the presence of such bubbles affects the mechanical strength and the structure of gassy marine sediments. The complexity of the problem means that all such theories will have limitations. The A&H theory contains inconsistencies in the frequency dependence of the expressions for the damping coefficients and scattering cross-sections.[27,28] It also involves a sign ambiguity in the sound speed formula.[4] Kargl *et al.*[24] investigated the double mono-pole resonance behavior of sediment-replacing gas bubbles, though they do not formulate the viscoelastic, acoustic, and thermal dissipation relevant to bubble pulsations. Leighton's theory for marine sediment bubble pulsations[3] lacked acoustic radiation losses, and he outlined the route for including them which Mantouka *et al.*[4] executed with, moreover, the formulation of nonlinear scattering. However, the rheological model for the sediment viscosity in Refs. 2 and 4 has some drawbacks, as will be explained in Sec. II.

At low driving frequencies, the bubble's response in a medium is stiffness-controlled[29] and the presence of bubbles

a)Electronic mail: t.g.leighton@soton.ac.uk

decreases the sound speed in that medium. In moving the driving frequency through resonance, a Pi phase change occurs in the bubble response. Consequently, at frequencies greater than resonance, the bubbles increase the sound speed.[30] At very high frequencies, far from resonance, the amplitude of bubble pulsation is small, and the sound speed values converge to those in the host medium (in this context, host medium refers to the fully water saturated sediment).[3,31] Clearly, the overall sound speed and attenuation in the medium depends on how the elastic moduli of the host medium are calculated. To do this, Gassmann's relations were employed in Refs. [1] and [2], and Berryman's self-consistent approximations[32,33] were used in Ref. [4]. Both of these methods are unable to predict the sound speed dispersion and the attenuation in the host medium, unless complex coefficients are introduced for the elastic moduli. In the present work, the effective density fluid model (EDFM), established by Williams[34] as an alternative to the Biot theory, is employed to describe wave propagation in the host medium. Its use allows incorporation of the dispersion and the dissipation of the first compressional wave in water-saturated sediment. The classical derivations for the dynamics of a pulsating bubble consider a single bubble fixed in space in an infinite body of liquid-like material.[3,31,35–37] However, Kargl[37] included the effect on the bubble in question of the multiple scattering from surrounding bubbles, when deriving the linear acoustics expressions. This paper includes multiple scattering in the same way.

Another objective of the present work is to demonstrate a general way of modeling the rheological effects near the bubble wall. When gas bubbles pulsate in marine sediment, shear (elastic) losses are induced outside of the gas-solid boundary, and viscous losses occur near the gas-liquid interface. In Ref. [2], an effective host medium (viscoelastic liquid) was assumed, and the elastic and viscous damping were combined into one by introducing a complex viscosity term. In Mantouka et al.,[4] the effective medium model was maintained. Although these two damping terms (elastic and viscous) were expressed separately, the sediment viscosity was deduced from the shear modulus, as in Ref. [2]. The latter approach has been used in several studies[38–40] to model the shear wave attenuation of water-saturated sediments. However, it leads to some discrepancies regarding the bubble resonance phenomenon when applied to gassy sediments (as will be shown in Sec. III). The current paper therefore keeps the general form of the constitutive equation in viscoelastic media as in Refs. [36] and [41–44], while it formulates the viscous and elastic losses separately by means of the porosity and the contact interfaces of the gas with the surroundings. Furthermore, the current paper proposes the use of sediment viscosity values obtained from rheological experiments.[45–49]

We should also note that the model presented here (and those in Refs. [3] and [4]) for acoustic propagation (the forward problem) can be used for the estimation of bubble void fraction and bubble size distribution in marine sediments (the inverse problem). The high attenuations exhibited by gassy marine sediments mean that, while most propagation theories are for steady-state low-amplitude pulsations, most experiments use high amplitude signals at short ranges

(meaning that signals are often short pulses). The formulations in Sec. II (and Refs. [3], [4], [50], and [51] on which they are based) allow simulation of the nonlinear, transient, and/or ring-down period of bubble oscillations when short high-amplitude acoustic pulses are used. This has not been possible with the steady-state theories. Similarly, the large bubble wall displacement and velocities during the high amplitude, high frequency insonification can be calculated using the methods described here (and in Refs. [3], [4], [50], and [51]), as well as the dynamics of bubbles driven with multiple frequency acoustic signals. Neither would have been possible using A&H theory.[1,2] These predictions could then be used to determine the time-dependent cloud response of bubbles, the sound speed, and the scattering cross sections as outlined in Refs. [50] and [51], which provides a general route for inverting such signals to characterize the bubble populations in marine sediments.

## II. FORMULATIONS

Consider the radial motion of a spherical gas bubble of radius $R(t)$ which is fixed in space and oscillates about some equilibrium radius $R_0$ with bubble wall velocity $\dot{R}(t)$. Assuming the flow is irrotational, the radial component of the equation for the conservation of momentum[36,52] can be written as

$$\rho_s \left( \frac{\partial v_r}{\partial t} + v_r \frac{\partial v_r}{\partial r} \right) = -\frac{\partial p}{\partial r} + \frac{\partial \tau_{rr}}{\partial r} + \frac{2}{r}[\tau_{rr} - \tau_{\theta\theta}], \quad (1)$$

where $\rho_s$ is the density of the water-saturated sediment, $v_r$ is the particle velocity in the sediment outside the bubble wall, $r$ denotes the distance from the centre of the bubble to an arbitrary location, and $\tau_{rr}$ and $\tau_{\theta\theta}$ are the stress components in $r$ and $\theta$ directions, respectively. Assuming for the moment that the solid and liquid phases are both incompressible, the velocity field in the vicinity of the bubble wall[31] can be found from

$$v_r = -\frac{\dot{R}(t)R^2(t)}{r^2}. \quad (2)$$

In Ref. [36], the medium surrounding the bubble was taken to be an effective homogeneous medium such that the pressure $p$ and the stresses have some equivalent average values. In the case of a porous medium (such as sediment), the bubble's surface has contact with the pore water and with the solid mineral grains, for which we establish symbols denoting the gas–liquid interface $\Omega_L$ and the gas–solid interface $\Omega_S$. Deresiewicz and Skalak[53] have shown that, for such an interface between a single phase (here, gas) and its poro-elastic surroundings (here, water and solid grains), the total area of $\Omega_L$ is proportional to the porosity $\beta$, and the area $\Omega_S$ is proportional to $1 - \beta$. The following boundary conditions on the bubble surface are then formulated

$$p_L(R,t)|_{\partial\Omega_L} - \tau_{rr}^L(R,t)|_{\partial\Omega_L} = p_g - \frac{2\sigma}{R} \quad \text{at } r = R, \quad (3)$$

$$-\tau_{rr}^S(R,t)|_{\partial\Omega_S} = p_g \quad \text{at } r = R, \quad (4)$$

where $p_g$ is the gas pressure inside the bubble, $p_L$ is the fluid pressure, $\sigma$ indicates the surface tension, and $\tau_{rr}^L$ and $\tau_{rr}^S$ represent the shear stresses in the liquid and in the solid, respectively.

At an intermediate distance, i.e., in the pore space and away from the bubble wall, the stress balance between the liquid and the solid is given by

$$p_L(r,t) - \tau_{rr}^L(r,t) = \tau_{rr}^S(r,t) \quad \text{at } r. \tag{5}$$

The pressure in the far field limit is defined as

$$p = p_0 \quad \text{at } r = \infty, \tag{6}$$

and we assume that the bubble wall is initially stationary and at the equilibrium position

$$R = R_0, \quad \dot{R} = 0 \quad \text{at } t = 0. \tag{7}$$

The integration of Eq. (1) through the whole volume of the sediment from the bubble wall at distance $R$ to a location $r$ in the near field gives

$$\int_R^r \rho_s \left( \frac{\partial v_r}{\partial t} + v_r \frac{\partial v_r}{\partial r} \right) dr$$
$$= -\int_R^r \int_{\Omega_L} \frac{\partial p}{\partial r} \, d\Omega \, dr + \int_R^r \int_{\Omega_L} \frac{\partial \tau_{rr}^L}{\partial r} \, d\Omega \, dr$$
$$+ \int_R^r \int_{\Omega_L} 3 \frac{\tau_{rr}^L}{r} \, d\Omega \, dr + \int_R^r \int_{\Omega_S} \frac{\partial \tau_{rr}^S}{\partial r} \, d\Omega \, dr$$
$$+ \int_R^r \int_{\Omega_S} 3 \frac{\tau_{rr}^S}{r} \, d\Omega \, dr. \tag{8}$$

Using the aforementioned relationships from Deresiewicz and Skalak,[53] integration over $\Omega_L$ results in terms proportional to $\beta$, and the integration over $\Omega_S$ results in terms proportional to $(1-\beta)$. Therefore, one can obtain

$$\rho_s \left( R\ddot{R} + \frac{3}{2}\dot{R}^2 \right) - \frac{\rho_s}{r}\dot{f} + \frac{\rho_s}{2}\frac{f^2}{r^4}$$
$$= -\beta \left[ p_L(R) - p_L(r) \right] + \beta \tau_{rr}^L \big|_R^r$$
$$+ \beta \int_R^r 3 \frac{\tau_{rr}^L}{r} \, dr + (1-\beta) \tau_{rr}^S \big|_R^r$$
$$+ (1-\beta) \int_R^r 3 \frac{\tau_{rr}^S}{r} \, dr. \tag{9}$$

Here the short-hand $f = R^2 \dot{R}$ has been introduced, and consequently the term $-\rho_s \dot{f}/r$ corresponds to the acoustic pressure radiated by a pulsating bubble at a distance $r$. Using the identity $p_{in} = p_L(r) - \tau_{rr}^L(r)$, it follows that

$$\rho_s \left( R\ddot{R} + \frac{3}{2}\dot{R}^2 \right) - \frac{\rho_s}{r}\dot{f} + \frac{\rho_s}{2}\frac{f^2}{r^4}$$
$$= p_{in} - \beta p_L(R) + \beta \tau_{rr}^L(R) + (1-\beta)\tau_{rr}^S(R)$$
$$+ \beta \int_R^\infty 3 \frac{\tau_{rr}^L}{r} \, dr + (1-\beta)\int_R^\infty 3 \frac{\tau_{rr}^S}{r} \, dr. \tag{10}$$

The far field acoustic propagation is modelled using the EDFM (Ref. 34) which is derived from Biot theory. The linear acoustic equation of the EDFM can be written as

$$\nabla^2 \varphi - \frac{1}{c_s^2}\frac{\partial^2 \varphi}{\partial t^2} = 0, \tag{11}$$

where $\varphi$ is the velocity potential, i.e., $\vec{v} = \nabla \varphi$, and $c_s^2 = H/\rho_s$ (the explicit expressions are given in the Appendix). The solution to Eq. (11) has the form

$$\varphi_{ex} = \frac{\psi_1}{r} e^{i\omega(t - r/c_s)}, \tag{12}$$

which characterizes an outgoing spherical wave. The expression for the far field pressure[54] is then given by

$$p_{ex} = p_0 - \rho_s \frac{\partial \varphi_{ex}}{\partial t}. \tag{13}$$

## A. Matching asymptotic solutions

In order to match the near field and far field solutions in the intermediate zone, the volumetric flow and the pressure matching conditions should be applied

$$4\pi r^2 v_{r(in)}\big|_{r\to\infty} = 4\pi r^2 v_{r(ex)}\big|_{r\to 0}, \quad p_{in}\big|_{r\to\infty} = p_{ex}\big|_{r\to 0}. \tag{14}$$

As $r \to \infty$, the bubble mediated acoustic pressure $\rho_s \dot{f}(t)/r$ and the quadratic term $\rho_s f^2/2r^4$ in Eq. (10) vanish.[36] Furthermore, the $r \to 0$ limit of the spherical wave in Eq. (12) induces a time-dependent acoustic driving pulse at the location of the bubble, i.e., $\partial \varphi_{ex}/\partial t\big|_{r\to 0} = P_A g(t)$, with $P_A$ being a positive real number that scales the driving pressure. Hence, the matching solutions for the pressure field give

$$\left(1 - \frac{\dot{R}}{c_s}\right) R\ddot{R} + \frac{3}{2}\left(1 - \frac{\dot{R}}{3c_s}\right)\dot{R}^2$$
$$= \left(1 + \frac{\dot{R}}{c_s}\right)\frac{p_L - p_\infty}{\rho_s} + \frac{R}{\rho_s c_s}\frac{d}{dt}(p_L - p_\infty), \tag{15}$$

where

$$p_L - p_\infty = p_g - \beta \frac{2\sigma}{R} - p_0 + P_A g(t)$$
$$+ \beta \int_R^\infty 3 \tau_{rr}^L / r \, dr + (1-\beta)\int_R^\infty 3 \tau_{rr}^S / r \, dr. \tag{16}$$

## B. Rheological constitutive relation

The Voigt model is appropriate for most marine sediments.[3,38,39,45] For a spherically symmetric flow, it is given by

$$\tau_{rr} = \tau_{rr}^S + \tau_{rr}^L = 2G\gamma_{rr} + 2\mu\dot{\gamma}_{rr}, \tag{17}$$

where $\gamma_{rr}$ and $\dot{\gamma}_{rr}$ are the strain and the strain rate in the radial direction, $G$ is the shear modulus, and $\mu$ denotes the

J. Acoust. Soc. Am. **141** (3), March 2017

Dogan *et al.* 2279

shear viscosity. In Eq. (17), a linear rheological model is imposed, i.e., the shear modulus and the viscosity are independent of $\gamma_{rr}$ and $\dot{\gamma}_{rr}$. The latter can be obtained using Eq. (2) as $\gamma_{rr} = -(2/3r^3)(R^3 - R_0^3)$ and $\dot{\gamma}_{rr} = -(2R^2/r^3)\dot{R}$. The integrals in Eq. (16) then can be calculated as

$$\beta \int_R^\infty 3\,\tau_{rr}^{\mathrm{L}}/r\,\mathrm{d}r + (1-\beta)\int_R^\infty 3\,\tau_{rr}^{\mathrm{S}}/r\,\mathrm{d}r$$
$$= -\beta\frac{4\mu\dot{R}}{R} - (1-\beta)\frac{4G}{3R^3}\left(R^3 - R_0^3\right). \tag{18}$$

Therefore, the Keller-Miksis type equation,[55] which describes the radial motion of a spherical bubble in an unbounded viscoelastic medium, can be written as

$$\rho_s\left(1 - \frac{\dot{R}}{c_s}\right)R\ddot{R} + \frac{3}{2}\rho_s\left(1 - \frac{\dot{R}}{3c_s}\right)\dot{R}^2$$
$$= \left(1 + \frac{\dot{R}}{c_s} + \frac{R}{c_s}\frac{\mathrm{d}}{\mathrm{dt}}\right) \times \left(p_g - \beta\frac{2\sigma}{R} - p_0 + P_A g(t)\right.$$
$$\left. -\beta\frac{4\mu\dot{R}}{R} - (1-\beta)\frac{4G}{3R^3}\left(R^3 - R_0^3\right)\right). \tag{19}$$

In order to complete the set of equations given above, the thermal physics related to the gas inside the bubble needs to be identified. This can be done comprehensively by solving the continuity and the energy conservation equations for a gas, as was one in Refs. 51 and 56. A less complicated, but often passably accurate alternative way of including the thermal dynamics of nonlinear gas bubbles, is to modify the polytropic law with an artificial thermal viscosity term $\mu_{\mathrm{th}}$,[56] i.e.,

$$p_g = p_{g_0}\left(\frac{R_0}{R}\right)^{3\kappa(\omega)} - 4\mu_{\mathrm{th}}\frac{\dot{R}}{R}, \tag{20}$$

where $p_{g_0}$ is the bubble gas pressure at the undisturbed state, $\kappa(\omega) = \mathrm{Re}(\Phi)$ is the polytropic exponent, $\mu_{\mathrm{th}} = (3p_{g_0}/4\omega)\mathrm{Im}(\Phi)$ is the thermal viscosity, and $\omega$ is the angular frequency. The variable $\Phi$ is given by

$$\Phi = \frac{\gamma}{1 - 3(\gamma-1)i\chi\left[\left(\frac{i}{\chi}\right)^{1/2}\coth\left(\frac{i}{\chi}\right)^{1/2} - 1\right]}, \tag{21}$$

where $\chi = D/\omega R_0^2$ represents the thermal diffusion length, with $D$ being the thermal diffusivity of the gas, and where $\gamma$ indicates the adiabatic polytropic exponent.

## C. Analytical solutions

An analytical solution to Eq. (19) may be obtained by assuming small perturbations of the bubble radius, i.e., $R = R_0(1 + x)$ where $x \ll 1$. The first order terms in $x$ are retained such that

$$\dot{R} = R_0\dot{x}, \tag{22a}$$

$$\ddot{R} = R_0\ddot{x}, \tag{22b}$$

$$R^{-1} = R_0^{-1}(1 - x), \tag{22c}$$

$$R^{-3\kappa} = R_0^{-3\kappa}(1 - 3\kappa x). \tag{22d}$$

Note that the incident pressure term is, to first order,[32,51] equivalent to the linear expression for the radiated pressure wave, as in

$$P_A g(t) = \frac{\rho_s\ddot{R}R_0}{\left(1 - \dfrac{i\omega R_0}{c_s}\right)}. \tag{23}$$

With this in mind, substitution of Eq. (22) into Eq. (19) allows the linearization of Eq. (19) in the radius-pressure frame of motion[31] to give

$$\ddot{x} + 2\beta_{\mathrm{tot}}\dot{x} + \omega_0^2 x = -\frac{P_A e^{i\omega t}}{m}, \tag{24}$$

where $\beta_{\mathrm{tot}}$ is the total damping, and the effective mass is

$$m = \rho_s R_0^2 + \frac{4\mu R_0}{c_s}. \tag{25}$$

Eliminating $e^{i\omega t}$ dependencies, Eq. (24) can be recast into a Helmholtz equation with the complex wavenumber

$$k_{\mathrm{m}}^2 = \frac{\omega^2}{c_s^2} + 4\pi\omega^2\int_0^\infty \frac{R_0 n(R_0)}{\omega_0^2 - \omega^2 + 2i\beta_{\mathrm{tot}}\omega}\,\mathrm{d}R_0, \tag{26}$$

where $n(R_0)\,\mathrm{d}R_0$ is the number of bubbles per unit volume with radii between $R_0$ and $R_0 + \mathrm{d}R_0$. The (viscous, thermal, acoustic, interfacial, and elastic) damping coefficients and the resonance frequency expression are obtained and take the following form:

$$\beta_{\mathrm{vis}} = 2\beta\mu/m, \tag{27a}$$

$$\beta_{\mathrm{th}} = \left(\frac{3p_{g_0}\mathrm{Im}(\phi)}{2\omega}\right)\Big/m, \tag{27b}$$

$$\beta_{\mathrm{ac}} = \frac{k_{\mathrm{m}}R_0}{1 + (k_{\mathrm{m}}R_0)^2}\frac{\omega}{2}, \tag{27c}$$

$$\beta_{\mathrm{int}} = -\frac{\beta\sigma}{mc_s}, \tag{27d}$$

$$\beta_{\mathrm{el}} = \frac{2G(1-\beta)R_0}{mc_s}, \tag{27e}$$

$$\omega_0^2 = \frac{\left[3p_{g_0}\mathrm{Re}(\phi) - \dfrac{2\sigma\beta}{R_0} + 4G(1-\beta) + \dfrac{\omega^2\rho R_0^2}{1 + (\omega R_0/c_s)^2}\right]}{m}. \tag{27f}$$

The last term in Eq. (26) represents the effects of bubbles on the acoustic propagation, whereas the complex quantity $\omega^2/c_s^2$ is the contribution from the dispersion and the dissipation in the host medium. Note that Eq. (26) should be calculated iteratively as in Ref. 37, because $\beta_{\mathrm{ac}}$ is a function of

$k_m$, in order to account for the higher order re-scattering from other bubbles.[37,57] The phase velocity $V$ and the attenuation $A$ (dB/m) are then related to the real and imaginary parts of the wavenumber, respectively, via

$$V = \omega / \mathrm{Re}\{k_m\} \tag{28}$$

and

$$A = 8.6859 \, |\mathrm{Im}\{k_m\}|. \tag{29}$$

### D. Linear expressions published previously

When modeling (gas-free) water-saturated sediments, some studies[58,59] have treated the medium as a lossy elastic solid using a complex shear modulus

$$\tau = G^*\gamma = (G - iG')\gamma. \tag{30}$$

Other approaches,[2,40] which are based on a viscoelastic liquid model, instead define a complex shear viscosity

$$\tau = \mu^*\dot{\gamma} = (\mu + i\mu')\dot{\gamma}. \tag{31}$$

The use of the algebraic relation $\dot{\gamma} = i\omega\gamma$, and the comparison of Eqs. (30) and (31), led historically to wide use[40,60,61] of

$$G^* = -i\omega\mu^*, \tag{32}$$

and to the use of $\mu' = G/\omega$ and $G' = \omega\mu$. Therefore, the complex viscosity in the equivalent liquid model is defined as $\mu^* = G'/\omega + i\mu'$. In Ref. 2, such a model was applied to gassy sediments.

The nondimensional viscous damping in a homogeneous liquid in the radius-force frame equation of motion[31] is given by

$$\delta_{vis} = \frac{4\mu}{\rho_s \omega R_0^2}. \tag{33}$$

By inserting into Eq. (33) the real part of the complex viscosity term given in Eq. (31), A&H followed Andreeva[62] to propose that the viscoelastic damping takes the following form:

$$\delta_{el}^{AH} = \frac{4G'}{\rho\omega^2 R_0^2}. \tag{34}$$

The imaginary part of the shear modulus in Eq. (34) is deduced from the shear wave attenuation in fully water-saturated sediment [e.g., some quasi-static values can be found as $G/G' \approx 5$ or $G/G' \approx 10$ (Ref. 25)]. The acoustic radiation damping $\delta_{ac}^{AH}$ given in Ref. 2 has been used by Lyons *et al.*[25] with the correction $\omega_0^2/\omega^2$ to the radiation damping, and Anderson (a co-author of Refs. 1, 2, and 25) is cited as a 2001 personal communication in Ref. 8 as advising Best *et al.*[8] to use the radiation damping factor of Ref. 25 not that of Ref. 2—this confusion was resolved by Ainslie and Leighton[27,28] who explained that Eqs. (55) and (56) of Ref. 1 are inconsistent with each other. A&H also neglect any

correction for the higher order scattering in the medium, which is formulated in this work via Eq. (27c).

The thermal damping constant, $\delta_{th}^{AH}$, of A&H is based on the analysis of Eller.[63] It will not be written explicitly here for brevity, but can be found in Refs. 2, 8, and 25. Eller's derivation is based on solving the heat conduction equation and is less comprehensive than formulas (20) and (21) based on energy conservation, as used here.

A&H follow Andreeva[62] in their expression for the resonance frequency, here multiplied by $2\pi$ and written in the polytropic limit

$$\omega_{0,AH} = \sqrt{(3\kappa p_{g_0} + 4G)/\rho R_0^2}. \tag{35}$$

The equations used by A&H, listed above, have some drawbacks mainly owing to the characteristics of their rheological model (31). First, the damping expression (34) assumes a $1/\omega$ dependence between the elastic and viscous responses of the sediment, and combines both dissipation mechanisms into one single term. In contrast, experimental studies[39,45–49] that have reported both the shear and the viscous properties (flow curves) of sediments do not suggest a straightforward $1/\omega$ dependence between the two. The elastic and the viscous responses may vary individually, depending on the strain amplitude and/or frequency ranges (in, for example, shear viscosity[58,59] and elastic modulus[61]). These may furthermore depend on the salinity, the mineralogical composition, and the concentration.[46,48] Second, there exists a discrepancy because of the use of $\mathrm{Re}(G^*)$ in the resonance frequency expression (35) and $\mathrm{Im}(G^*)$ in the damping coefficient (34). This, in turn, results in a mismatch between the resonance frequency and the frequency at which minimum damping occurs, creating an inconsistency in terms of the resonance phenomenon.

### III. RESULTS

The results obtained by applying the current theory to the marine sediments are presented and compared to those obtained by the A&H model, and with the predictions of Mantouka *et al.*[4] Figures 1 and 2 plot the damping coefficients, Fig. 3 the sound speeds, and Figs. 4 and 5 the attenuation results. Two different sediment types, ocean silt and harbor mud, are examined (to assist comparisons, the parameter values are the same as those used by A&H,[2] as listed in Table I). The value of bubble gas volume fraction ($\Gamma$) in Figs. 3 and 4 is taken as 0.075% for harbor mud and as 0.068% for ocean silt, which were the void fractions used by A&H, so that the two acoustical models can be compared. The A&H model did not include viscosity, but values are required for our model, and chosen here in order to resemble an increasingly viscous behavior as the porosity increases. A value of 2.52 MPa was reported for the shear modulus for the sediment sample in Ref. 8, and 26 MPa for the sediment sample in Ref. 34. Based on this range of values, we choose 1 and 26 MPa shear modulus values for mud and silt, respectively. Also note that $G'$, $\rho$, and $c_s$ in Table I are the constant values required by A&H, whereas the Appendix to this paper shows how the frequency-dependent values of $\rho_s$ and $c_s$ are calculated for the current theory. This nomenclature has

J. Acoust. Soc. Am. **141** (3), March 2017
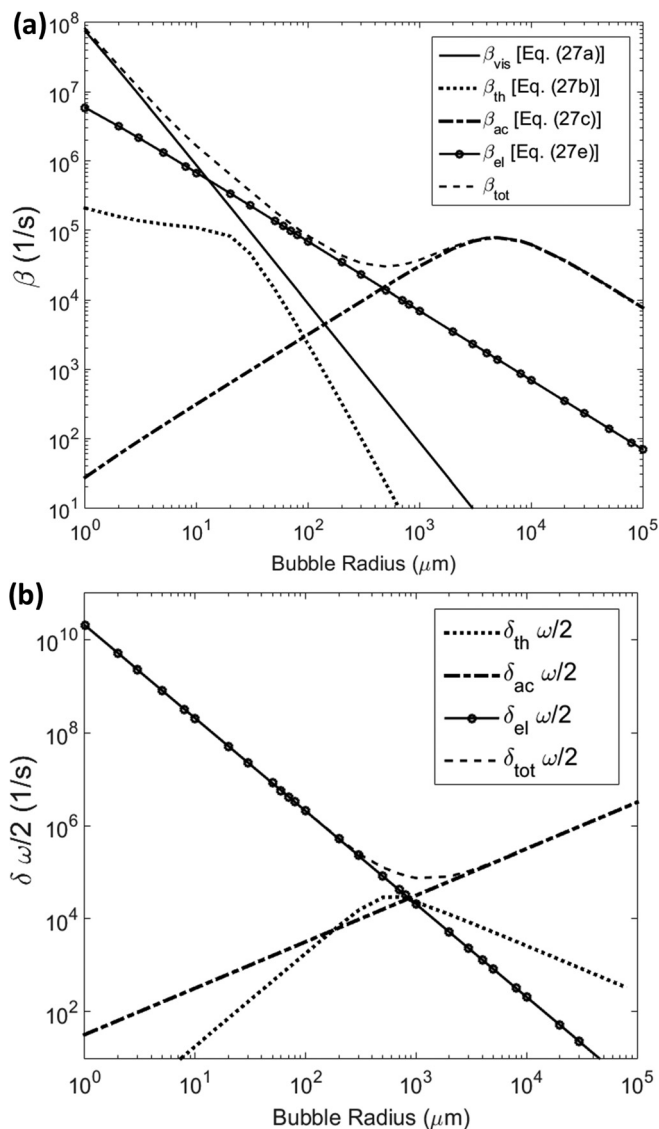
Dogan *et al.* 2281

FIG. 1. Damping coefficients vs equilibrium bubble radius in ocean silt at a pulse frequency of 50 kHz by using (a) the current formulation and (b) A&H formulation. In (a) the dimensional damping coefficients are given in Eq. (27). In (b) the non-dimensional coefficients are multiplied by $\omega/2$ for conversion. $\delta_{el}$ is given in Eq. (34). The expressions for $\delta_{th}$ and $\delta_{ac}$ can be found in Ref. 2.
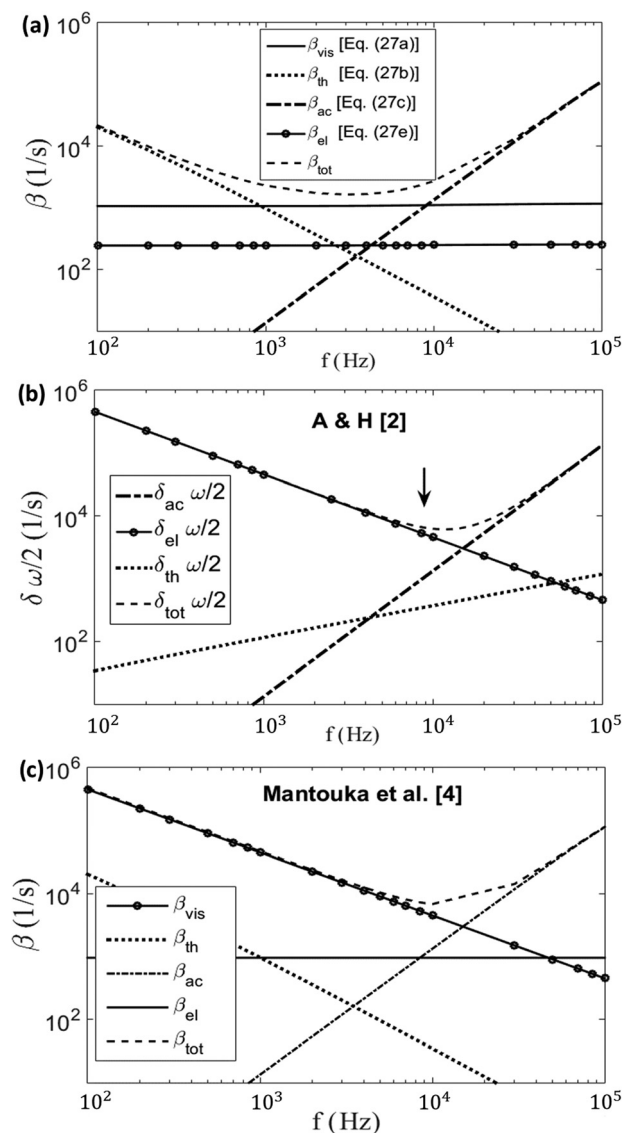


FIG. 2. Damping coefficients vs driving frequency for a 1 mm equilibrium radius bubble in mud by using (a) the current formulation, (b) A&H formulation and (c) Ref. 4. In (b), the arrow indicates the resonance frequency calculated using Eq. (35).

been adopted to save introducing a new variable but accommodate the fact that when A&H theory is used, the density and sound speed take constant values (here, given in Table I). However, the theory of this paper calculates frequency-dependent values for both (note that in each case, the theories of A&H and this paper refer to the same physical quantity). Although A&H do not use the theory in the Appendix, nevertheless Eq. (A4) requires use of Eq. (A5), and the values chosen in Table I for the density are consistent with Eq. (A5).

## A. Damping coefficients

Five different physical mechanisms contribute to the damping (Sec. II C). The values of damping coefficients given in Eq. (27) versus bubble radius for a fixed driving frequency are shown in Fig. 1(a) for ocean silt. The predictions

of the A&H theory given by Eqs. (34) and (35) are also plotted in Fig. 1(b). Note that the damping coefficient in Eq. (34) is in non-dimensional form and $\beta$ in the current formulation is the dimensional damping coefficient, therefore for conversion $\delta$ values are multiplied by $\omega/2$.

Three significant ranges appear in Fig. 1(a), where different types of damping become the dominant loss mechanism according to the current formulation. As in the case of bubbles in water, viscous damping is the dominant loss mechanism for small bubble sizes. The values obtained for the viscous damping are a few orders of magnitude higher than viscous dissipation in water (not shown in the figure), as a consequence of the higher viscosities of mud- and clay-like sediments. Both formulations demonstrate that acoustic damping is the most effective loss mechanism for bubbles over 1 mm in radius. For intermediate bubble radii ($\sim 100\,\mu m$), the thermal damping based on Prosperetti's formulation [Fig. 1(a)] is about 2 orders of magnitude higher

2282    J. Acoust. Soc. Am. **141** (3), March 2017
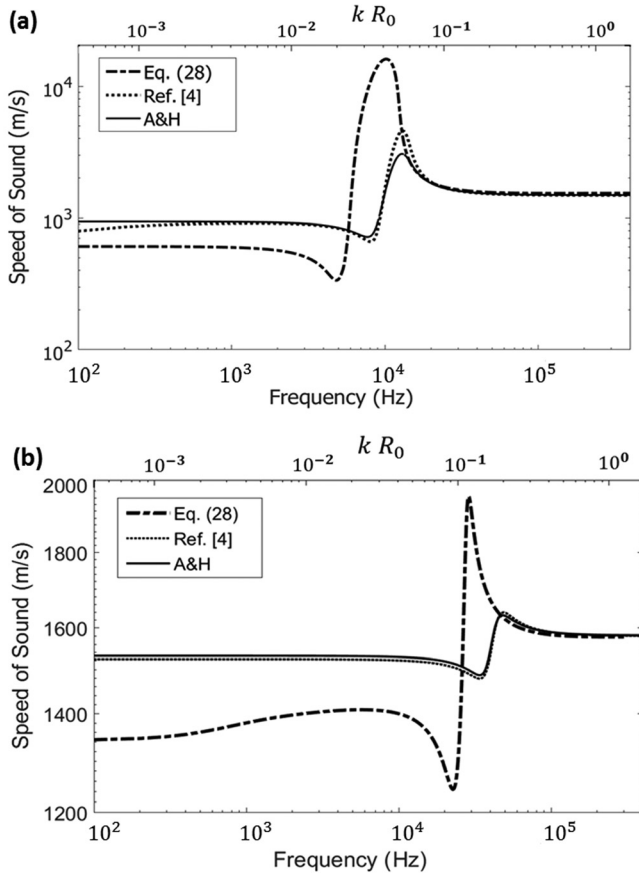
Dogan *et al.*

**(a)**

**(b)**

FIG. 3. Speed of sound through a mono-disperse bubble population $R_0 = 1$ mm in (a) harbor mud for $\Gamma = 0.075\%$, and (b) ocean silt for $\Gamma = 0.068\%$. They are plotted using the current formulation, Ref. 4, and the A&H theory. The dimensionless wavenumber $kR_0$ is plotted on the top axis in order to place the data in the context of the long wavelength assumption used in linear theories.

than the one predicted by Eller's formulation [Fig. 1(b)]. One can show that thermal losses may be the most pronounced dissipation for medium sized bubbles in more fluid-like sediments such as mud.
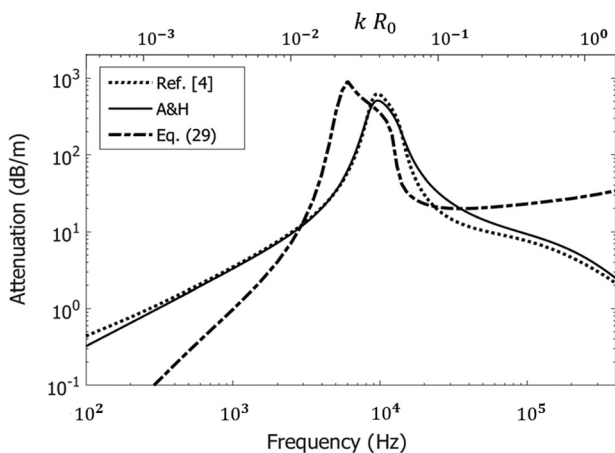


FIG. 4. Attenuation of an acoustic wave through a mono-disperse bubble population with $R_0 = 1$ mm in harbor mud plotted by using the current formulation, Ref. 4, and the A&H theory for bubble gas fraction of 0.075%. The dimensionless wavenumber $kR_0$ is 0.1 at 23.8 kHz, however the $x$ axis is extended to 400 kHz in order to display the evolution of the curves.
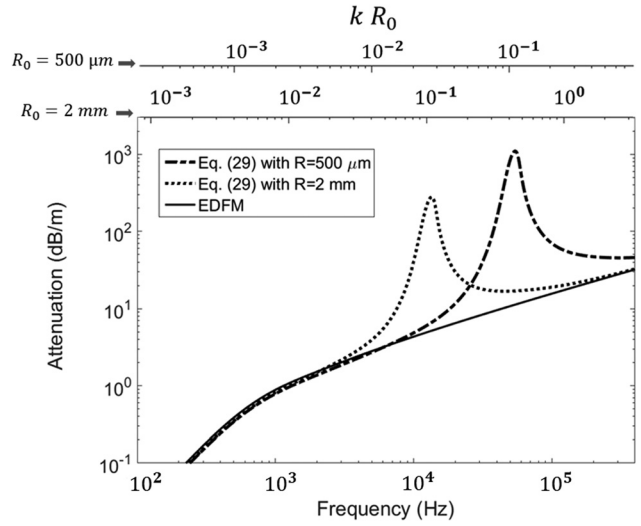
FIG. 5. Attenuation of acoustic wave through a mono-disperse bubble population in ocean silt plotted by using the current formulation for bubble gas fraction 0.1%. The solid black line shows the results from the EDFM for gas free sediment. The dimensionless wavenumber $kR_0$ is shown along the top axis for 500 $\mu$m and 2 mm bubbles.

At the largest bubble sizes shown, the radiation damping coefficient increases with increasing bubble size in Fig. 1(b), but not in Fig. 1(a) (which affects the behavior of the total damping coefficient at large bubble sizes). This arises because of the $(kR_0)^2$ in Eq. (27c) that was originally derived by Yang and Church.[36] At the other end of the radius range, for the smallest bubble sizes shown, the thermal damping coefficient increases with decreasing bubble size in Fig. 1(a), but not in Fig. 1(b). This is because of Eller's simplifications in describing thermal dissipation via the heat conduction equation route[63] [used in Fig. 1(b)] rather than basing it on energy conservation[56] [used in Fig. 1(a)].

The elastic damping given in Eq. (27e) decays linearly with the equilibrium bubble radius $R_0$. The viscoelastic dissipation predicted in Fig. 1(b) is about 2 orders of magnitude higher at the 10–100 $\mu$m range where elastic damping is the most effective. This may be attributed to the combined viscoelastic damping term $\delta_{el}^{AH}$. The interfacial damping,

TABLE I. Model input parameters for harbor mud and ocean silt. To allow direct comparison, the values to be used in Figs. 1–4 were chosen to be the same as in Ref. 2. Note that A&H did not include sediment viscosities, which for our model are selected from the range stated in Refs. 47 and 49, choosing values that allow the mud under consideration to be more fluid-like than the silt.

|  | Harbor mud | Ocean silt |
|---|---|---|
| Porosity | 0.75 | 0.68 |
| Shear modulus ($G$) | 1 MPa | 26 MPa (Ref. 34) |
| $G'$ (Imaginary part of $G^*$) | 0.2 MPa | 5.2 MPa |
| Bubble void fraction ($\Gamma$) | 0.00075 (0.075%) for Figs. 3(a) and 4 | 0.00068 (0.068%) for Fig. 3(b); 0.001 (0.1%) for Fig. 5 |
| Total mass density ($\rho$) | 1410 kg/m$^3$ | 1530 kg/m$^3$ |
| Speed of sound ($c_s$) | 1480 m/s | 1552 m/s |
| Viscosity ($\mu$) (Refs. 47 and 49) | 1 Pa s | 0.1 Pa s |

Eq. (27d), has a negligible contribution to the total damping,[4] and hence it is omitted from the plots for clarity.

The formulations of Mantouka et al.[4] would give thermal coefficient identical to those in Fig. 1(a), and the viscoelastic coefficient identical to that in Fig. 1(b).

The results for the damping coefficients as a function of insonifying frequency are shown in Fig. 2 for a bubble of 1 mm radius in mud. The major causes of the losses are thermal and acoustic damping, the former being the most important at frequencies below resonance, and the latter being more effective above the resonance frequency of the bubble. The viscous and the elastic damping terms are independent of frequency in the size range plotted for the present formulation [Eqs. (27a) and (27e)]. The $\delta_{el}^{AH}$ values are high in the 0.1–10 kHz range, and are inversely proportional ($1/\omega$) to the drive frequency. Consequently, the A&H model predicts very high attenuation in the low seismic frequency range ($\sim$1–100 Hz) (which will be shown in Fig. 4), but this is not observed in practical applications.[15,16,64] The arrow shown in Fig. 2(b) identifies the bubble resonance frequency expressed in Eq. (35). The indication is that the resonance frequency does not coincide with the frequency at which the minimum damping occurs.

In Fig. 2(c), the damping coefficients are also compared with the ones derived in Mantouka et al.[4] [Eqs. (20a)–(20f) of that paper]. The viscoelastic damping in Ref. 4 and in Ref. 2 are identical (after the multiplication of the latter by $\omega/2$), because the complex shear modulus approach was also employed in Ref. 4, citing the viscoelastic model in Ref. 2. The thermal damping [Eq. (20b)] in Ref. 4 is identical with the one presented in the current paper [Eq. (27b)]. The elastic damping Eq. (20e) in Ref. 4 is multiplied by a factor of $1 - \beta$ in Eq. (27e) to account for poroelastic boundary conditions between the gas, the solid, and the liquid. Similarly, the interfacial damping in the present text [Eq. (27d)] has a correction factor $\beta$ compared to the one derived in Ref. 4, owing to the poroelastic boundary conditions used instead of the homogeneous medium approach. Furthermore, the acoustic radiation damping in the present work is re-expressed to account for the multiple scattering, the effects of which will now be demonstrated in Figs. 3 and 4.

## B. Speed of sound

The speed of sound in gassy sediments is plotted in Fig. 3(a) for bubbles in harbor mud. Note that the gas void fraction $\Gamma$ is not formulated in terms of an implicit percentage in Ref. 2, i.e., a value of $\Gamma = 0.01$ in Ref. 2 refers to 1% bubble void fraction. Typical values of $\Gamma$ observed in practice are in the range $\sim$1%–2%[25,65] (see Leighton and Robb[66] for a detailed list). The dashed-dotted line in Fig. 3 reproduces the result obtained by the current formulation for harbor mud with the gas void fraction value $\Gamma = 0.075\%$. The solid line gives the results of A&H theory and the dotted line presents the result from the formulation in Mantouka et al.[4] At the high frequency limit, the predictions of A&H and Mantouka et al.[4] converge to the sound speed value in saturated sediment (1480 m/s), whereas the current model predicts 1540 m/s owing to the phase velocity dispersion

observed in the fast wave. Similarly, at low frequencies the previous theories[2,4] converge to a value such that, as the decreasing frequency takes the pulsation further from the bubble resonance, the sound speed becomes primarily a function of the bulk modulus of the host medium and bulk modulus of the gas.[66] These effects, and those associated with the transition from below-resonance to above-resonance, are markedly different between the current formulation and its predecessors. The reasons for this are the corrections to the damping coefficients and the resonance frequency (the multiplication of $G$ with $1 - \beta$), and the velocity dispersion caused by the incorporation of the EDFM. The effects of the multiple scattering are also evident through the increased phase velocity values, as were also seen in water.[37] The dimensionless wavenumber $kR_0$ is shown along the top axis in Fig. 3 in order to assess the long wavelength assumption ($kR_0 \ll 1$) used in Sec. II, and in the previous studies.[2,4] The value of $kR_0$ is 0.1 at 23.8 kHz and here the high frequency asymptotic behavior is reached at about 30 kHz. However, in the following it will be shown that this criterion is not always met, especially in sediments with higher shear modulus. The implications of that will be discussed below.

Wave propagation through a monodisperse bubble cloud in ocean silt is also examined for a gas void fraction of 0.068% [Fig. 3(b)]. Although previous formulations[1,2,4] show a small effect due to this bubble population, Eq. (28) shows additional dispersion in the low frequency limit and through-resonance regime, because of the movement of the pore fluid.[15–17,34] Even so, the effects on sound speed caused by gas bubble pulsations are relatively small in a sediment with such a high rigidity [see Fig. 3(a) in Ref. 4], compared to the effects observed in a more fluid-like sediment such as mud in Fig. 3(a). The reason may be attributed to the relatively small bulk modulus of the gas in this case, so that the bubbles are acoustically less effective in altering the sound speed. The low frequency limit of the sound speed ($c_s^{LF}$) in Figs. 3(a) and 3(b) can indeed be closely predicted by the Mallock-Wood equation[67] for the sound speed in suspensions

$$c_s^{LF} = \left( \rho_g \, \Gamma + \rho_s \, [1 - \Gamma] \right)^{-1/2} \left( \frac{\Gamma}{B_g} + \frac{1 - \Gamma}{\rho_s c_s^2} \right)^{-1/2}, \quad (36)$$

where $\rho_g$ is the density of the gas. The bulk modulus of the gas $B_g$ can be calculated for low frequency–low amplitude pulsations as[68]

$$B_g \approx -\rho_s R_0^2 \, \omega_0^2/3, \quad (37)$$

with $\omega_0^2$ being given in Eq. (27f) of this paper. For instance, the sound speed value at 100 Hz for muddy sediment is calculated in this way as 597 m/s compared to the value of 635 m/s in Fig. 3(a), and the sound speed value at 100 Hz for silt example is calculated as 1325 m/s compared to the value 1344 m/s in Fig. 3(b). These calculations and the low and high frequency limits of the sound speed can be observed in more detail in the supplementary material[69] that accompanies this paper (see Figs. E1 and E2 therein).

## C. Attenuation

The values of attenuation in gassy sediments are plotted in Figs. 4 and 5 for bubbles in harbor mud and ocean silt, respectively. The gas void fraction is taken as 0.075% for harbor mud. The dashed line in Fig. 4 gives the result obtained by Eq. (29) for harbor mud. The current formulation predicts lower attenuation in harbor mud for pulse frequencies less than 3 kHz, though the attenuation peak is higher than those of A&H and Mantouka et al.[4] in the near-resonance regime for the current mono-disperse bubble population. The current formulation suggests that a significant correction is required (compared to the theories of Refs. 2 and 4) when predicting the resonance frequency, primarily because of the multiplication factor $1 - \beta$ in Eq. (27f). Moreover, the broader nature of the curve obtained with Eq. (29) is due to the multiple scattering from other bubbles. A similar effect has been observed in gassy water.[37] Although, at the highest frequencies in Fig. 4, the present and previous[2,4] formulations appear to disagree qualitatively, in this range $kR_0$ is no longer $\ll 1$ and so inferences drawn in this regime are of limited value. However, the trend is for Eq. (29) to follow the attenuation for water-saturated sediment above resonance (a liquid viscosity effect that is not captured by the existing formulations[2,4]). This can be attributed to the incorporation of the EDFM.

Figure 5 shows the computed values of attenuation for different bubble radii in ocean silt assuming a gas void fraction value of $\Gamma = 0.1\%$. This is higher than that used in Figs. 3 and 4 and Ref. 2, in order to emphasize the bubble-induced effects in ocean silt. The solid black line indicates the results from the EDFM, which corresponds to the attenuation in saturated sediment (without gas bubbles). The dotted line shows the attenuation in gassy sediment with monodisperse bubble population with $R_0 = 2$ mm, and the dashed line with $R_0 = 500 \, \mu$m. The peaks coincide with the corresponding resonance frequencies for these bubble radii. As with Fig. 4, above resonance the EDFM ensures that the gassy sediment attenuation curve follows that for water-saturated sediment, and Refs. 2 and 4 lack this feature.

The formulation presented here can readily be extended to polydisperse bubble populations. Such characteristic curves will aid the planning of experiments to measure the bubble size distribution and the total bubble void fraction using acoustic inversion methods.

The $kR_0$ values are shown along the top axis in Fig. 5 for the given bubbles sizes. The long wavelength assumption inherent in the linear theory begins to break down at around the resonance frequency for each bubble size in Fig. 5. This shows that, while the theories can be used to make predictions outside of the long wavelength limit, they must be treated with care. This is particularly germane for ocean sediments if, say, one attempts to invert acoustic information to estimate the bubble population present. Prior to a measurement, the experimenter does not know the maximum size of a bubble in his acoustic field that the sediment has stabilized. It is unrealistic to select some large $R_0$ a priori and restrict the acoustic frequencies to the $kR_0 \ll 1$ range. That policy would restrict the available acoustic frequency range so much that it would severely compromise the information that can be taken. This illustrates the conflict inherent in gassy ocean sediment acoustics, in that the possible presence of large stabilized bubbles means that the experimental frequency range and long-wavelength theoretical limitations must be critically assessed.

## IV. CONCLUSIONS

A method for acoustic propagation in gassy marine sediments is presented. The formulation incorporates the EDFM for the host medium. Not surprisingly, it predicts that such a medium exhibits high attenuation near the bubble resonance frequencies. However, in the high frequency limit, the attenuation also increases to values that resemble those observed in gas-free sediments, owing to the viscous dissipation in the pore fluid. The latter phenomenon has not been captured by previous formulations written for this class of work, i.e., sediment-replacing gas bubbles. The phase velocity shows significant dispersion caused by the presence of both the pore fluid and the gas bubbles. It has been shown that the high frequency sound speed limit of the formulation in the present paper approaches that of EDFM. Furthermore, the low frequency sound speed limit of the present paper can be closely predicted by the Mallock-Wood equation for suspensions, provided that the low frequency sound speed value of the EDFM and the expressions in the current paper for the bulk modulus of the gas are used in the calculations. Supplementary material[69] with two additional figures (see Figs. E1 and E2 therein), which validate these calculations, accompanies this paper.

The paper further focused on the constitutive effects observed near the bubble interface. The rheological model used here accounts for the contact surfaces between the phases individually, rather than assuming an effective homogeneous host medium. Consequently, new expressions are derived for the viscous [Eq. (27a)], interfacial [Eq. (27d)], and elastic damping [Eq. (27e)] and for the resonance frequency [Eq. (27f)]. These differ from those of Mantouka et al.[4] {the expressions of Yang and Church [Eqs. (23) and (24) in Ref. 36] were for soft tissue and lacked porosity terms}. Moreover, the effects of the multiple scattering are included through Eq. (27c). The general conclusions are that the viscous and elastic losses dominate at small bubble radii, and the effect of the surface tension at the gas-liquid interface is negligible. A thermal damping formulation, based on energy conservation, is provided. This may be an important loss mechanism at intermediate bubble sizes in mud- and clay-like sediments. The acoustic radiation damping clearly becomes very effective with increasing driving frequencies and larger bubble radii. Multiple scattering from other bubbles broadens the attenuation peaks and elevates the phase velocity near the bubble resonance, resembling the effects they cause in gassy water.[37]

The current work assumed that the stress was linearly related to the strain, in keeping with the assumption of a Voigt relationship. While this is an adequate assumption for sediments with low gas void fractions driven by low amplitude acoustic pulses, real sediments may exhibit a frequency-dependent viscous and/or elastic behavior.[58,59,61] This effect could be readily included in the current

J. Acoust. Soc. Am. **141** (3), March 2017

Dogan *et al.* 2285

formulation, because the incorporation of a frequency-dependent shear modulus and viscosity is straightforward through Eq. (17). It should also be noted that in the case of high amplitude pulses, alternative constitutive equations (e.g., as in Refs. 58, 70, and 71) may be required. These would allow the stress-strain variables to scale with $\gamma^n$ and $\dot{\gamma}^n$ (the exponent $n$ being not necessarily equal to 1). These rheological models can be formulated within the framework presented here with modifications to the integrals in Eq. (18).

## APPENDIX

The wave equation of the EDFM (Ref. 34) is given by

$$k_{\text{eff}}^2 H \varphi = \omega^2 \rho_s \varphi, \tag{A1}$$

where $H$ is related to the bulk modulus of sand grains $K_r$ and the bulk modulus of the pore fluid $K_f$ with

$$H = \left( \frac{1-\beta}{K_r} + \frac{\beta}{K_f} \right)^{-1}. \tag{A2}$$

The complex sound speed in the sediment is then

$$c_s = \sqrt{H/\rho_s}, \tag{A3}$$

where

$$\rho_s = \left( \frac{\alpha(1-\beta)\rho_m + \beta(1-\alpha)\rho_f + i\dfrac{\beta\rho F \mu_f}{\rho_f \kappa \omega}}{\beta(1-\beta)\rho_m + (\alpha - 2\beta + \beta^2)\rho_f + i\dfrac{\beta F \mu_f}{\omega \kappa}} \right). \tag{A4}$$

In Eq. (A4), $\alpha$ is the tortuosity, $\mu_f$ denotes the viscosity of the pore fluid, $\rho_m$ is the density of the mineral grains, $\rho_f$ is the density of the pore fluid, and the total mass density is given by

$$\rho = (1-\beta)\rho_m + \beta\rho_f. \tag{A5}$$

The pore size parameter $a$ is defined as

$$a = \sqrt{\frac{8\alpha\kappa}{\beta}}, \tag{A6}$$

with $\kappa$ being the permeability. The parameter $F$ represents the viscous shear dissipation in the pore fluid during the high frequency oscillations and can be found from

$$F(\epsilon) = \frac{\epsilon \dfrac{T(\epsilon)}{4}}{1 - 2i\dfrac{T(\epsilon)}{\epsilon}}, \tag{A7}$$

with

$$T(\epsilon) = \frac{-\sqrt{i}\, J_1\left(\epsilon\sqrt{i}\right)}{J_0\left(\epsilon\sqrt{i}\right)}, \tag{A8}$$

where $J_1$ and $J_0$ are cylindrical Bessel functions and

$$\epsilon = \sqrt{\frac{\omega \rho_f}{\mu_f}}. \tag{A9}$$

The following values were used when calculating the EDFM equations: $K_r = 5 \times 10^{10}\,\text{Pa}$, $K_f = 2.3 \times 10^9\,\text{Pa}$, $\rho_m = 2650\,\text{kg/m}^3$, $\rho_f = 1000\,\text{kg/m}^3$, $\mu_f = 0.001\,\text{Pa s}$, $\kappa = 1.0 \times 10^{-10}\,\text{m}^2$, and $\alpha = 1.25$.

[1]A. L. Anderson and L. D. Hampton, "Acoustics of gas-bearing sediments. I. Background," J. Acoust. Soc. Am. **67**(6), 1865–1889 (1980).

[2]A. L. Anderson and L. D. Hampton, "Acoustics of gas-bearing sediment. II. Measurements and models," J. Acoust. Soc. Am. **67**(6), 1890–1903 (1980).

[3]T. G. Leighton, "Theory for acoustic propagation in marine sediment containing gas bubbles which may pulsate in a non-stationary nonlinear model," Geophys. Res. Lett. **34**, L17607, doi:10.1029/2007GL030803 (2007).

[4]A. Mantouka, H. Dogan, P. R. White, and T. G. Leighton, "Modelling acoustic scattering, sound speed, and attenuation in gassy soft marine sediments," J. Acoust. Soc. Am. **140**, 274–282 (2016).

[5]A. I. Best, M. D. Richardson, B. P. Boudreau, A. G. Judd, I. Leifer, A. P. Lyons, C. S. Martens, D. L. Orange, and S. J. Wheeler, "Shallow bed methane gas could pose coastal hazard," EOS Trans. **87**(22), 213–217 (2006).

[6]I. M. Brooks, M. J. Yelland, R. C. Upstill-Goddard, P. D. Nightingale, S. Archer, E. D'Asaro, R. Beale, C. Beatty, B. Blomquist, A. A. Bloom, B. J. Brooks, J. Cluderay, D. Coles, J. Dacey, M. DeGrandpre, J. Dixon, W. M. Drennan, J. Gabriele, L. Goldson, N. Hardman-Mountford, M. K. Hill, M. Horn, P.-C. Hsueh, B. Huebert, G. de Leeuw, T. G. Leighton, M. Liddicoat, J. J. N. Lingard, C. McNeil, J. B. McQuaid, B. I. Moat, G. Moore, C. Neill, S. J. Norris, S. O'Doherty, R. W. Pascal, J. Prytherch, M. Rebozo, E. Sahlee, M. Salter, U. Schuster, I. Skjelvan, H. Slagter, M. H. Smith, P. D. Smith, M. Srokosz, J. A. Stephens, P. K. Taylor, M. Telszewski, R. Walsh, B. Ward, D. K. Woolf, D. Young, and H. Zemmelink, "Physical exchanges at the Air Sea Interface: UK SOLAS field measurements," Bull. Am. Meteorol. Soc. **90**(5), 629–644 (2009).

[7]T. G. Leighton and P. R. White, "Quantification of undersea gas leaks from carbon capture and storage facilities, from pipelines and from methane seeps, by their acoustic emissions," Proc. R. Soc. A **468**, 485–510 (2012).

[8]A. I. Best, M. D. J. Tuffin, J. K. Dix, and J. M. Bull, "Tidal height and frequency dependence of acoustic velocity and attenuation in shallow gassy marine sediments," J. Geophys. Res. **109**(B8), B08101, doi:10.1029/2003JB002748 (2004).

[9]J. Blackford, H. Stahl, J. Bull, B. Berges, M. Cevatoglu, A. Lichtschlag, D. Connelly, R. James, J. Kita, D. Long, M. Naylor, K. Shitashima, D. Smith, P. Taylor, I. Wright, M. Akhurst, B. Chen, T. Gernon, C. Hauton, M. Hayashi, H. Kaieda, T. G. Leighton, T. Sato, M. Sayer, M. Suzumura, K. Tait, M. Vardy, P. R. White, and S. Widdicombe, "Detection and impacts of leakage from sub-seafloor deep geological carbon dioxide storage," Nature Climate Change **4**(11), 1011–1016 (2014).

2286   J. Acoust. Soc. Am. **141** (3), March 2017

Dogan *et al.*

[10]B. J. P. Berges, T. G. Leighton, and P. R. White, "Passive acoustic quantification of gas fluxes during controlled gas release experiments," Int. J. Greenhouse Gas Control 38, 64–79 (2015).

[11]M. A. Biot, "Theory of propagation of elastic waves in fluid-saturated porous solids: I. Low-frequency range," J. Acoust. Soc. Am. 28(2), 168–178 (1956).

[12]M. A. Biot, "Theory of propagation of elastic waves in fluid-saturated porous solids: II. Higher frequency range," J. Acoust. Soc. Am. 28(2), 179–191 (1956).

[13]T. J. Plona, "Observation of a second compressional wave in a porous medium at ultrasonic frequencies," Appl. Phys. Lett. 36(4), 259–261 (1980).

[14]D. L. Johnson and T. J. Plona, "Acoustic slow waves and the consolidation transition," J. Acoust. Soc. Am. 72, 556–565 (1982).

[15]R. D. Stoll and G. M. Bryan, "Wave attenuation in saturated sediments," J. Acoust. Soc. Am. 47(5), 1440–1447 (1970).

[16]R. D. Stoll, "Experimental studies of attenuation in sediments," J. Acoust. Soc. Am. 66(4), 1152–1160 (1979).

[17]R. D. Stoll, "Marine sediment acoustics," J. Acoust. Soc. Am. 77(5), 1789–1799 (1985).

[18]A. Bedford and M. Stern, "A model for wave propagation in gassy sediments," J. Acoust. Soc. Am. 73(2), 409–417 (1983).

[19]J. A. Hawkins and A. Bedford, "Variational theory of bubbly media with a distribution of bubble sizes. 2: Porous solids," Int. J. Eng. Sci. 30(9), 1177–1186 (1992).

[20]J. L. Buchanan, "A comparison of broadband models for sand sediments," J. Acoust. Soc. Am. 120(6), 3584–3598 (2006).

[21]D. M. J. Smeulders and M. E. H. Van Dongen, "Wave propagation in porous media containing a dilute gas-liquid mixture," J. Fluid Mech. 343, 351–373 (1997).

[22]V. E. Nakoryakov and V. E. Dontsov, "Pressure waves in porous medium saturated with liquid containing gas bubbles," J. Eng. Mech. 131, 966–973 (2005).

[23]M. A. Biot, "Generalized theory of acoustic propagation in porous dissipative media," J. Acoust. Soc. Am. 34(9), 1254–1264 (1962).

[24]S. G. Kargl, K. L. Williams, and R. Lim, "Double monopole resonance of a gas-filled, spherical cavity in a sediment," J. Acoust. Soc. Am. 103(1), 265–274 (1998).

[25]A. P. Lyons, M. E. Duncan, and A. L. Anderson, "Predictions of the acoustic scattering response of free-methane bubbles in muddy sediments," J. Acoust. Soc. Am. 99(1), 163–172 (1996).

[26]G. B. N. Robb, T. G. Leighton, J. K. Dix, A. I. Best, V. F. Humprey, and P. R. White, "Measuring bubble populations in gassy marine sediments: A review," Proc. Inst. Acoust. 28, 60–68 (2006).

[27]M. A. Ainslie and T. G. Leighton, "Near resonant bubble acoustic cross-section corrections, including examples from oceanography, volcanology, and biomedical ultrasound," J. Acoust. Soc. Am. 126(5), 2163–2175 (2009).

[28]M. A. Ainslie and T. G. Leighton, "Review of scattering and extinction cross-sections, damping factors, and resonance frequencies of a spherical gas bubble," J. Acoust. Soc. Am. 130(5), 3184–3208 (2011).

[29]T. G. Leighton, "From seas to surgeries, from babbling brooks to baby scans: The acoustics of gas bubbles in liquids," Int. J. Modern Phys. B 18(25), 3267–3314 (2004).

[30]T. G. Leighton, "What is ultrasound?," Prog. Biophys. Molecular Biol. 93(1–3), 3–83 (2007).

[31]T. G. Leighton, The Acoustic Bubble (Academic, London, 1994).

[32]J. G. Berryman, "Long-wavelength propagation in composite elastic media I. Spherical inclusions," J. Acoust. Soc. Am. 68(6), 1808–1819 (1980).

[33]J. G. Berryman, "Long-wavelength propagation in composite elastic media II. Ellipsoidal inclusions," J. Acoust. Soc. Am. 68(6), 1820–1831 (1980).

[34]K. L. Williams, "An effective fluid density model for acoustic propagation in sediments derived from Biot theory," J. Acoust. Soc. Am. 110(5), 2276–2281 (2001).

[35]K. W. Commander and A. Prosperetti, "Linear pressure waves in bubbly liquids: Comparison between theory and experiment," J. Acoust. Soc. Am. 85, 732–746 (1989).

[36]X. Yang and C. C. Church, "A model for dynamics of gas bubbles in soft tissue," J. Acoust. Soc. Am. 118(6), 3595–3606 (2004).

[37]S. G. Kargl, "Effective medium approach to linear acoustics in bubbly liquids," J. Acoust. Soc. Am. 111(1), 168–173 (2002).

[38]J. P.-Y. Maa and A. J. Mehta, "Soft mud response to water waves," J. Waterway, Port, Coastal, Ocean Eng. 116(5), 634–650 (1990).

[39]J. P.-Y. Maa and A. J. Mehta, "Soft mud properties: Voigt model," Waterway, Port, Coastal, Ocean Eng. 114(6), 765–770 (1988).

[40]H. Macpherson, "The attenuation of water waves over a non-rigid bed," J. Fluid Mech. 97(4), 721–742 (1980).

[41]C. C. Church, "The effects of an elastic solid surface layer on the radial pulsations of gas bubbles," J. Acoust. Soc. Am. 97(3), 1510–1521 (1995).

[42]A. A. Doinikov and P. A. Dayton, "Spatio-temporal dynamics of an encapsulated gas bubble in an ultrasound field," J. Acoust. Soc. Am. 120(2), 661–669 (2006).

[43]D. B. Khismatullin and A. Nadim, "Radial oscillations of encapsulated microbubbles in viscoelastic liquids," Phys. Fluids 14(10), 3534–3557 (2002).

[44]E. A. Zabolotskaya, Y. A. Ilinskii, G. D. Meegan, and M. F. Hamilton, "Modifications of the equation for gas bubble dynamics in a soft elastic medium," J. Acoust. Soc. Am. 118(4), 2173–2181 (2005).

[45]Z. Huang and H. Aode, "A laboratory study of rheological properties of mudflows in Hangzhou Bay, China," Int. J. Sediment Res. 24(4), 410–424 (2009).

[46]M. Sultanpour and F. Samsami, "A comparative study on the rheology and wave dissipation of kaolinite and natural Hendjian Coast mud, the Persian Gulf," Ocean Dyn. 61, 295–309 (2011).

[47]T. Van Kessel and C. Blom, "Rheology of cohesive sediments: Comparison between a natural and an artificial mud," J. Hydraul. Res. 36(4), 591–612 (1998).

[48]S. A. Haghshenas and M. Sultanpour, "An analysis of wave dissipation at the Hendjian Coast mud, the Persian Gulf," Ocean Dyn. 61, 217–232 (2011).

[49]W. Y. Hsu, H. H. Hwung, T. J. Hsu, A. Torres-Freyermuth, and R. Y. Yang, "An experimental and numerical investigation on wave-mud interactions," J. Geophys. Res.: Oceans 118(3), 1126–1141, doi:10.1002/jgrc.20103 (2013).

[50]J. W. L. Clarke and T. G. Leighton, "A method for estimating time-dependent acoustic cross-sections of bubbles and bubble clouds prior to the steady state," J. Acoust. Soc. Am. 107(4), 1922–1929 (2000).

[51]T. G. Leighton, S. D. Meers, and P. R. White, "Propagation through non-linear time-dependent bubble clouds and the estimation of bubble populations from measured acoustic characteristics," Proc. R. Soc. London A 460(2049), 2521–2550 (2004).

[52]L. D. Landau and E. M. Lifshitz, Fluid Mechanics, 2nd ed. (Pergamon, Oxford, 1987).

[53]H. Deresiewicz and R. Skalak, "On uniqueness in dynamic poro-elasticity," Bull. Seismol. Soc. Am. 53, 783–789 (1963).

[54]A. Prosperetti and A. Lezzi, "Bubble dynamics in a compressible liquid. Part 1. First-order theory," J. Fluid Mech. 168, 457–478 (1986).

[55]J. B. Keller and M. J. Miksis, "Bubble oscillations of large amplitude," J. Acoust. Soc. Am. 68, 628–633 (1980).

[56]A. Prosperetti, L. Crum, and K. Commander, "Nonlinear bubble dynamics," J. Acoust. Soc. Am. 83, 502–514 (1988).

[57]F. S. Henyey, "Corrections to Foldy's effective medium theory for propagation in bubble clouds and other collections of very small scatterers," J. Acoust. Soc. Am. 105(4), 2149–2154 (1999).

[58]H.-T. Chou, M. A. Foda, and J. R. Hunt, "Rheological response of cohesive sediments to oscillatory forcing," in Nearshore and Estuarine Cohesive Sediment Transport, Coastal Estuarine Science Series 42, Washington, D.C., AGU (2013), pp. 126–147.

[59]M. A. Foda, J. R. Hunt, and H.-T. Chou, "A nonlinear model for the fluidization of marine muds by waves," J. Geophys. Res. 98(C4), 7039–7047, doi:10.1029/92JC02797 (1993).

[60]J. D. Ferry, Viscoelastic Properties of Polymers (John Wiley & Sons, New York, 1980).

[61]M. Jain and A. J. Mehta, "Role of basic rheological models in determination of wave attenuation over muddy seabeds," Cont. Shelf Res. 29, 642–651 (2009).

[62]I. B. Andreeva, "Scattering of sound by air bladders of fish in deep sound-scattering ocean layers," Sov. Phys. Acoust. 10, 17–20 (1964).

[63]A. I. Eller, "Damping constants of pulsating bubbles," J. Acoust. Soc. Am. 47, 1469–1470 (1970).

[64]E. L. Hamilton, "Compressional wave attenuation in marine sediments," Geophys. 37, 620–646 (1972).

[65]Z. Toth, V. Spiess, J. M. Mogollon, and J. B. Jensen, "Estimating the free gas content in Baltic Sea sediments using compressional wave velocity

J. Acoust. Soc. Am. 141 (3), March 2017

Dogan et al.    2287

from marine seismic data," J. Geophys. Res.: Solid Earth **119**, 8577–8593, doi:10.1002/2014JB010989 (2014).

[66]T. G. Leighton and G. Robb, "Preliminary mapping of void fractions and sound speeds in gassy marine sediments from subbottom profiles," J. Acoust. Soc. Am. **124**(5), EL313–EL320 (2008).

[67]A. B. Wood and D. E. Weston, "The propagation of sound in mud," Acustica **14**, 156–162 (1964).

[68]T. G. Leighton, "A method for estimating sound speed and the void fractions of bubbles from sub-bottom sonar images of gassy seabeds," ISVR Technical Report No. 320, Southampton UK (2007), 30 pp.

[69]See supplementary material at http://dx.doi.org/10.1121/1.4978926 for calculations to check the low frequency limit of the sound speed with the predictions of EDFM.

[70]H. S. Fogler and J. D. Goddard, "Collapse of spherical cavities in visco-elastic liquids," Phys. Fluids **13**(5), 1135–1141 (1970).

[71]J. G. Oldroyd, "On the formulation of rheological equations of state," Proc. R. Soc. London A **200**, 523–541 (1950).

2288    J. Acoust. Soc. Am. **141** (3), March 2017

Dogan *et al.*